Forest Attributes from Radar Interferometric Structure and Its Fusion with Optical Remote Sensing

ROBERT N. TREUHAFT, BEVERLY E. LAW, AND GREGORY P. ASNER

The possibility of global, three-dimensional remote sensing of forest structure with interferometric synthetic aperture radar (InSAR) bears on important forest ecological processes, particularly the carbon cycle. InSAR supplements two-dimensional remote sensing with information in the vertical dimension. Its strengths in potential for global coverage complement those of lidar (light detecting and ranging), which has the potential for high-accuracy vertical profiles over small areas. InSAR derives its sensitivity to forest vertical structure from the differences in signals received by two, spatially separate radar receivers. Estimation of parameters describing vertical structure requires multiple-polarization, multiple-frequency, or multiple-baseline InSAR. Combining InSAR with complementary remote sensing techniques, such as hyperspectral optical imaging and lidar, can enhance vertical-structure estimates and consequent biophysical quantities of importance to ecologists, such as biomass. Future InSAR experiments will supplement recent airborne and spaceborne demonstrations, and together with inputs from ecologists regarding structure, they will suggest designs for future spaceborne strategies for measuring global vegetation structure.

Keywords: remote sensing, carbon cycle, InSAR, lidar, optical remote sensing, forest ecology

Important ecological processes are expressed in and are affected by the vertical structure of forest canopies. Chief among these processes is the carbon cycle, the uncertainties in which limit understanding of climatic trends over the next century. Changes in vegetation structure, induced by climatic conditions, natural disturbance, and human activities, can have substantial impacts on carbon storage and the exchange of carbon dioxide (CO_2), water vapor, and heat with the atmosphere (Law et al. 2001), which can modify climate (Pielke and Avissar 1990).

Trees store carbon in their biomass. Fossil fuel burning and deforestation, which release carbon as CO_2 into the atmosphere, are believed to be the two dominant contributing mechanisms to the rise in atmospheric CO_2 over the last 50 years. Forest biomass also has a potential role in reabsorbing some of the excess CO_2, yet the dynamic responses of carbon fluxes to climate changes are still poorly understood. Knowledge of the level of carbon stored in forest biomass globally is highly uncertain (within about 40% of the true value; Waring and Running 1998), as is the spatiotemporal description of carbon flux associated with changes in aboveground biomass. Improved quantification of biomass will help reduce uncertainty in estimates of magnitudes, rates, and longevity of carbon sequestration by terrestrial ecosystems (Law et al. forthcoming), and therefore will enable better understanding of the global carbon cycle. In this article, we demonstrate quantification of, and magnitudes of uncertainties in, carbon sequestration; we also discuss scaling issues and the need for improving model estimates with data assimilation.

Biomass may be most robustly determined from remotely sensed, three-dimensional (3-D) forest structure (Lefsky et al.

Robert N. Treuhaft (e-mail: robert.treuhaft@jpl.nasa.gov) is a research scientist at the Jet Propulsion Laboratory, California Institute of Technology, Pasadena, CA 91109. Beverly E. Law is an associate professor in the College of Forestry, Oregon State University, Corvallis, OR 97331, who specializes in ecophysiology and ecosystem processes. Gregory P. Asner is a research scientist in the Carnegie Institution's Department of Global Ecology and in the Department of Geological and Environmental Sciences, Stanford University, Stanford, CA 94305.

1999, Drake et al. 2002, Treuhaft et al. 2003). Estimates of this 3-D structure result from augmenting two-dimensional (2-D) remote sensing with vertical structure measurements. Accurate 3-D structure estimates over regions and continents are needed to determine the role of terrestrial ecosystems in the global carbon cycle. Regrowth and the consequent biomass accumulation following stand-replacing disturbances, such as fire and deforestation, induce vertical-structure changes potentially accessible to 3-D remote sensing. Other forest disturbances, such as insect outbreaks, windthrow, and selective timber harvesting, present more subtle structural signatures that may also be detected by new 3-D remote sensing approaches (Marchak 1995). Neither the rates and extents of thinning-type disturbances nor the patterns of forest recovery are well known at large spatial scales. These disturbances, however, play critical roles in determining the carbon balance and ecological functioning of forest ecosystems (Waring and Running 1998, Law et al. 2003).

Within the last decade, experimental demonstrations of the 3-D techniques of interferometric synthetic aperture radar (InSAR) (Graham 1974) and lidar ([laser] light detecting and ranging) (Gardner 1992) have suggested the possibility of remotely sensing global 3-D vegetation structure. Demonstrations of vegetation-structure sensitivity and estimation include InSAR (Hagberg et al. 1995, Treuhaft et al. 1996, 2002, Cloude and Papathanassiou 1998) and lidar (Nilsson 1996, Lefsky et al. 1999, Drake et al. 2002) experiments. Both InSAR and lidar 3-D techniques show potential to measure canopy attributes accurately in the vertical as well as horizontal directions. This article explains how InSAR works and describes its potential to measure canopy structure in three dimensions, primarily for global forest vegetation profiling. Other articles describe the ecological applications of lidar (Lefsky et al. 2002), of noninterferometric synthetic aperture radar (SAR) (Waring et al. 1995), and of multispectral (Cohen and Goward 2004) and hyperspectral (Ustin et al. 2004) optical remote sensing. The 3-D biophysical description of forests is complex, and its global description will no doubt require more than one remote sensing technique. For that reason, this discussion has a secondary focus on InSAR's enhanced utility when combined with other sensors in so-called data fusion.

From 2-D to 3-D remote sensing: InSAR and lidar

First we contrast generic 2-D, power-based remote sensing approaches with the additional measurements made to observe the third, vertical dimension with InSAR. We also compare the capabilities and limitations of InSAR and lidar to establish a context for InSAR 3-D remote sensing. In either microwave SAR or optical 2-D remote sensing, the strength of the signal (power) received by a sensor is the sum of the powers attributed to each canopy element. Active sensors, such as radar and lidar, send out a pulse of radiation in selected wavelengths and measure the power of the reflected signal. Passive sensors (multispectral and hyperspectral) rely on the sun's energy and capture the changes in radiance (power at optical wavelengths) of a few or many spectral bands that are associated with the properties of the soil surface and vegetation.

The 2-D signals from two vegetation elements, such as a collection of leaves and twigs (depicted as green hexagons), originate at two different heights above the ground surface (figure 1a). The power sent by each vegetation element to the sensor (shown as vectors in the inset boxes) depends on how

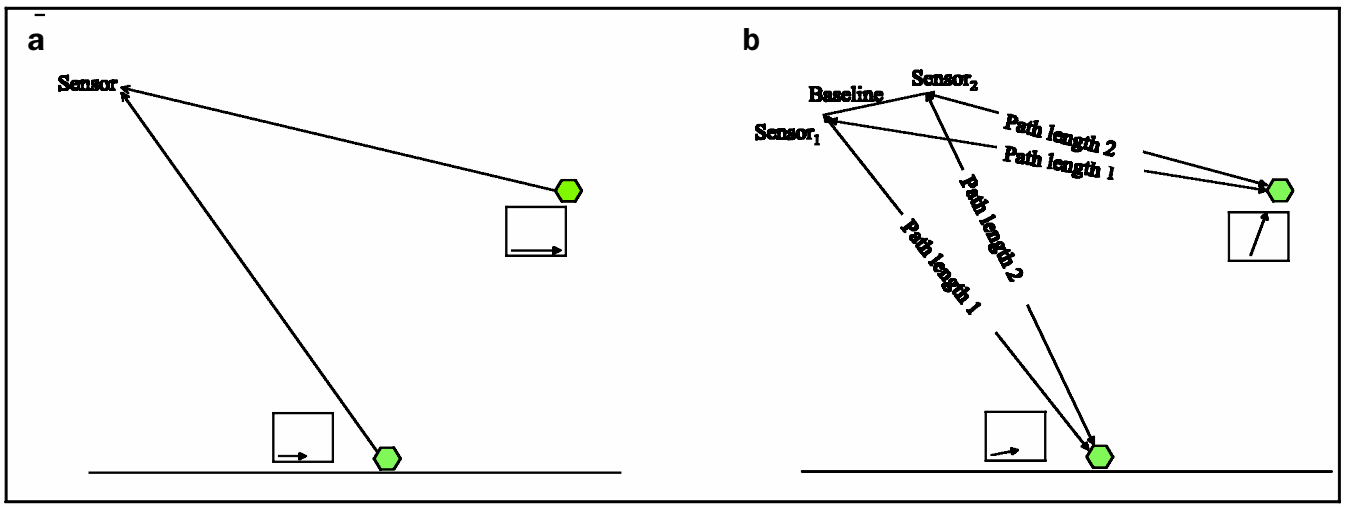

Figure 1. Distinction between two-dimensional (2-D) and three-dimensional (3-D) remote sensing of canopy elements. (a) 2-D: The return signals to a sensor from short and tall canopy elements, depicted as green hexagons above the forest floor, contribute to the total signal with information only on the strengths of the canopy elements, not their altitudes above the surface. (b) 3-D: With signals acquired at two ends of a baseline, the vertical location of canopy elements can be detected. The length of the vectors (within the boxes) indicates the power of the signal returned from each element; departure in angle from horizontal is proportional to path length 1 minus path length 2, which is proportional to the height above the surface, as well as to the InSAR phase for each element.

individual structures within the element redirect radiation toward the sensor, as well as the number of scattering structures per unit volume (number density). If we could somehow label the vertical position from which the power of each element originated, we would have a measurement that directly depends on number density profile, which correlates with biophysical densities of interest to ecologists (e.g., leaf area or mass density). Because the powers from each element add together in the total-power signal without a clear vertical-position label (indicated with horizontal vectors, which are added in figure 2), the vertical position of each element's number density is lost when blended into the total power 2-D measurement. That is, profiles cannot be directly estimated.

Beyond received power, InSAR (Treuhaft et al. 1996, Rosen et al. 2000) and lidar (Lefsky et al. 2002) each measure something more, a vertical label of sorts, which can be used to estimate properties in the third dimension. InSAR senses the heights of the vegetation elements via the interferometric phases (explained in the next section). Lidar senses the round-trip travel time associated with the power from vegetation elements, which also depends on vertical position.

The characteristics that differentiate the two 3-D techniques are spatiotemporal coverage and accuracy. Microwaves, which make radar images, penetrate clouds and can instantaneously cover large track widths (swaths) on the earth of about 80 kilometers (km) with current technology. The Shuttle Radar Topography Mission (SRTM, a spaceborne InSAR mission in 2000) (Rabus et al. 2003) provided gapless global, fixed-baseline InSAR coverage between the latitudes of ±60 degrees in 11 days. Although its primary mission was topographic, SRTM was the first seamless, global, spaceborne mission directly sensitive to 3-D vegetation structure. Plans for the repeat-track InSAR operation of the Advanced Land Observing Satellite (or ALOS, to be launched in 2004) (Igarashi 2001) make large-swath, all-weather, spaceborne InSAR possible in the near future. Because a spaceborne lidar, such as the previously proposed Vegetation Canopy Lidar (VCL) (Hofton et al. 2002), would acquire data only in clear conditions and have a swath width less than 100 meters (m), only about 2% of the globe could be sampled annually, so that gapless global coverage using lidar would require 50 years. A lidar used only in part for vegetation, now flying on the Ice, Cloud, and Land Elevation Satellite (or ICESat), has similar swath characteristics (Zwally et al. 2002). The biggest advantage of InSAR over lidar is in the tropics, which account for about 45% of the world's forest biomass (Schlesinger 1991), because in some tropical locations, cloud cover is so extensive that optical sensors may not acquire data as often as once per month, and, in some cases, may acquire data less than once per year (Asner 2001).

On the other hand, lidar's profiling accuracy is superior to that of InSAR. Although a detailed comparison of the profiling accuracy of each technique has yet to be done, validations of InSAR (Treuhaft et al. 2002) and lidar (Harding et al. 2001) with respective field measurements show that lidar captures all salient features of the vertical profiles, while InSAR captures only dominant features, smoothing over some features and producing more coarse profiles. Current InSAR lateral resolution for profiles is about 0.25 to 1 hectare (ha) (100 m × 100 m), while the VCL lateral resolution is of the order of 0.05 ha. Moreover, lidar can achieve its higher accuracy with a single measurement from one sensor; InSAR requires more than one measurement and possibly more than one sensor, and in most cases it produces less accurate vertical and horizontal resolution than lidar. With current technology, InSAR's potential for global spatiotemporal coverage exceeds that of lidar by approximately three orders of magnitude, but it comes at the expense of spaceborne hardware costs and vertical profile accuracy. Ideally, global InSAR and lidar can be combined to optimize spatiotemporal coverage and accuracy.

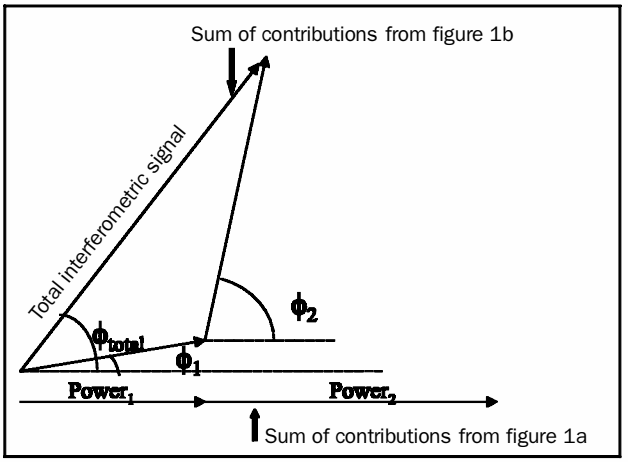

Figure 2. Interpreting the signal from two canopy elements with InSAR. Assuming the same vertical placement of elements as in figure 1, the phases ϕ_1 and ϕ_2 are similar to the insets in figure 1b and proportional to the height of each element above the ground. Power$_1$ is the amplitude from the lower element (length of the vector at angle ϕ_1 to the horizontal and the length of the horizontal power vector on the bottom), and Power$_2$ is the amplitude from the upper element. The amplitude of the total interferometric signal, signified by the vector's length, is smaller than the sum of powers shown at the bottom because canopy elements at different heights add vectorially in InSAR. The total InSAR phase, ϕ_{total}, is between ϕ_1 and ϕ_2.

3-D remote sensing with InSAR

InSAR was originally conceived as a bare-surface topography tool (Graham 1974), but the rich signatures of 3-D vertical complexity in InSAR data soon prompted interest in InSAR as a vegetation structure tool for ecosystem monitoring. InSAR draws from a long history of the use of interferometry to measure the structure of objects. In astronomy, for example, interferometric measurements of the structure of celestial objects date from the early part of the 20th century to the present (Thompson et al. 1986). The capability of InSAR to estimate vegetation structure follows from its

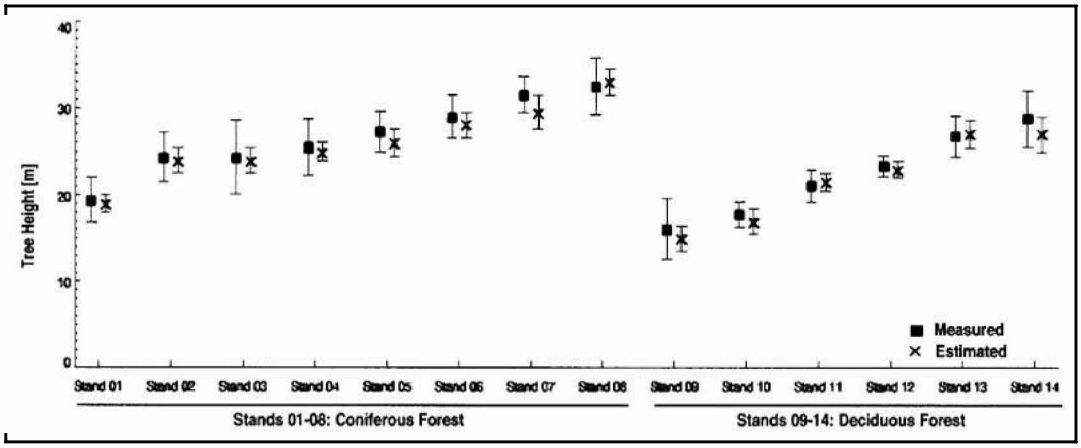

Figure 3. Comparison of field (measured, dark rectangles) and remotely sensed (estimated, crosses) tree heights from single-baseline polarimetric InSAR at Oberpfaffenhofen, Germany. The first eight stands are evergreen coniferous; the last six are deciduous broadleaf. Vertical lines represent one standard error. Reprinted from Papathanassiou and Cloude (2001), with permission. © 2001 Institute of Electrical and Electronics Engineers.

satisfying two criteria, which, we suggest, any set of remote sensing observations must meet to determine a given terrestrial attribute: The observations must (1) be sensitive to changes in that attribute and (2) yield unambiguous estimates of the parameters describing the attribute. If changes in distinct attributes of land surfaces induce similar signals, which may be misinterpreted, criterion 1 is met but criterion 2 is not. The descriptions of InSAR in the next sections show that single-baseline InSAR meets criterion 1 for 3-D vegetation structure, and several types of multiple-observation InSAR meet criteria 1 and 2. Both performance criteria must be met to remotely sense forest structure from space.

Criterion 1: InSAR's sensitivity to vegetation profiles. A radar interferometer has two sensors, or receivers, spatially separated at each end of a baseline (figure 1b). Two receivers make a "fixed baseline." Fixed-baseline InSAR has been demonstrated from the air with the NASA airborne synthetic aperture radar (AIRSAR) (Treuhaft et al. 1996, Treuhaft and Siqueira 2000, Slatton et al. 2001) and from space with SRTM (Rabus et al. 2003). In contrast, "repeat-track" InSAR synthesizes a baseline from a receiver flown repeatedly over an area (Hagberg et al. 1995, Wegmüller and Werner 1997, Papathanassiou and Cloude 2001). Platforms used in spaceborne repeat-track vegetation experiments include the Shuttle Imaging Radar (Cloude and Papathanassiou 1998) and JERS-1 (Japanese Earth Resource Satellite) and European Remote Sensing (ERS) satellites (Luckman et al. 2000, Pulliainen et al. 2003, Wagner et al. 2003).

For either fixed-baseline or repeat-track InSAR, there are two interferometric observations per baseline, the InSAR phase and amplitude. The phase is proportional to the path length difference from the vegetation element to each receiver, path length 1 minus path length 2 (figure 1b). This path length difference is in turn proportional (to a close approximation) to the vegetation's height above the surface, that is, path length 1 minus path length 2 is greater for the higher vegetation element in the figure. Extending the baseline accentuates the differences in phase between altitudes. The phase is the vertical-position label with which each vegetation element's contribution enters the total InSAR signal. The amplitude for each element is the same as the radar power for that element (figure 1a), and it depends on the power due to the elements as seen through the intervening forest. Note, however, that the InSAR signals (designated by vectors in inset boxes in figure 1b) depart from the horizontal with angles proportional to the InSAR phase, or height, above the ground surface; as before, the length of each vector expresses the power. (The fact that InSAR signals can be represented and added vectorially is a result of electromagnetic propagation and signal processing [Rodriguez and Martin 1992, Treuhaft et al. 1996].)

These vectors add quite differently (see the vector diagram, figure 2) from the 2-D linear case (the horizontal line at the bottom of figure 2). The two vegetation elements, with altitudes and amplitudes as in figures 1a and 1b, have InSAR phases ϕ_1 and ϕ_2 in figure 2. The vector sum, or the total InSAR observation resulting from these two elements, has a phase, ϕ_{total}, between ϕ_1 and ϕ_2. The ratio of the total InSAR amplitude to the 2-D total power (coherence) is always less than 1. A signal coming from a tall canopy is more "incoherent" than one coming from a shorter one. Thus, interferometry is sensitive in two ways to the vertical extent of vegetation: The InSAR phase generally increases, while the coherence decreases, the more vertically distributed the vegetation.

Criterion 2: InSAR's capability to estimate vegetation. The interferometric phase and coherence respond to the vertical distribution of vegetation, but many different element combinations could produce the same total InSAR amplitude and phase (figure 2). This means that while single-baseline

InSAR depends on structure profiles (criterion 1)—each element has entered into the signal with its phase, or altitude label—it cannot estimate the vertical vegetation profiles ecologists need (criterion 2). The reason for failing criterion 2 is that four parameters (the power and altitude of each vegetation element) cannot be extracted with only two single-baseline observations (phase and coherence). The number of profile-sensitive interferometric observations must match or exceed the number of parameters needed to describe the profile. Profiles can be estimated only when the observation set is expanded beyond single-baseline InSAR.

Multiple-polarization (the vector direction of the electric field in a plane perpendicular to its direction of propagation), multiple-frequency, or multiple-baseline observations each enable some level of profile estimation (heights or full profiles). To see how the profile information is recovered, think of each of the altitudes of our two vegetation elements as different colors of paint. Each color is concealed in a closed can. In this analogy, a single InSAR measurement corresponds to a given mixture of the colors, say a 1:2 ratio from the two cans (the single vector diagram of figure 2 is one mixture of altitudes). If can A contains red and can B blue, then the 1:2 mixture would be violet. Changing the polarization, frequency, or baseline in a known way systematically changes the mixture of altitudes, which is like changing the mixture of colors from 1:2 to, say, 2:1, resulting in a different color, perhaps magenta. From the colors of these two mixtures, we can probably deduce that the colors in cans A and B are close to red and blue; this is analogous to estimating the altitude parameters from multiple-observation InSAR, which can only infer the underlying altitude distribution from multiple mixtures. Lidar is more direct than InSAR and, in this analogy, lidar separately opens up each can and looks inside.

Profiles of interest to ecologists are more complex than the two-element example, but they usually result from a model involving a small number of parameters, depending on the assumed profile. InSAR models are based on empirical correlation (Wagner et al. 2003) or on physical descriptions of the vegetation (Papathanassiou and Cloude 2001). The model assumption of a uniform layer up to a maximum height suggests estimating a tree height (one parameter) from InSAR data. Assuming a Gaussian vegetation distribution suggests estimating the mean and standard deviation of a vertical Gaussian density distribution (two parameters). With increasing complexity in the assumed forest, the number of parameters increases, requiring increasing interferometric or other observations beyond the single-baseline observation. All models usually include the altitude of the underlying surface, the topography, as a parameter. The complexity of the assumed distribution depends on the particular ecological question being addressed by the profile information and on the type of forest observed. The multiple-polarization, multiple-frequency, and multiple-baseline strategies described below enable estimation of parameters in simple profile models.

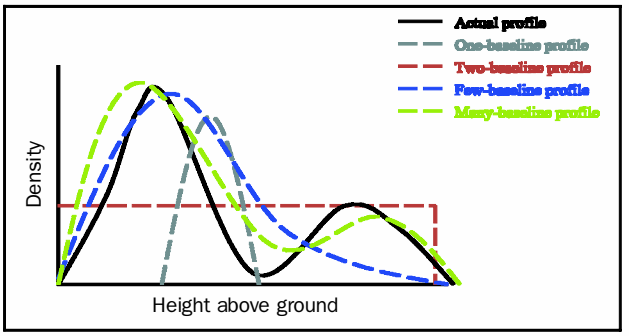

Figure 4. Conceptual drawing showing how the vertical detail of profiles improves with increasing numbers of baselines. With only one baseline, only an effective height and width of the distribution of vegetation can be determined from phase and coherence measurements. With two baselines, the mean height of a uniform stand can be discerned. With additional baselines, measurements come progressively closer to the actual underlying canopy profile.

Multiple-polarization, or polarimetric interferometry. Each unique combination of transmitted and received polarization yields different mixtures of the vegetation heights represented in the total InSAR signal. By "different mixtures" we mean adding vegetation vectors (as in figure 2) with different strengths or amplitudes, which depend on vegetation density. Components of a forested landscape that have a definite orientation, such as the horizontally oriented ground, have a distinct response to each polarization combination, usefully augmenting the observation set. A collection of leaves oriented in many random directions would probably induce very similar received signals, regardless of the polarization. If oriented, polarimetrically sensitive objects exist in the scene, polarimetric interferometry can be used to meet criterion 2 for simple model profiles (Cloude and Papathanassiou 1998, Treuhaft and Siqueira 2000, Papathanssiou and Cloude 2001). Figure 3 shows the results of applying a polarimetric, uniform-layer model to estimate tree heights, using polarimetric interferometry to augment the single-polarization, single-baseline observation set (Papathanassiou and Cloude 2001). The ground is the polarimetrically sensitive object in the model, and the root mean square error between remote sensing and ground height measurements is about 2 m.

Multiple-frequency interferometry. Radar interferometric observations at different frequencies also yield a diverse observation set from which profile information may be extracted. Models usually assume that returns from higher frequencies are from the top of the canopy and from smaller objects such as leaves, while returns from the lower frequencies involve a combination of the ground and larger canopy objects such as branches or trunks.

InSAR data at two frequencies, P-band (wavelength of approximately 70 centimeters [cm]) and X-band (wavelength of approximately 2 cm), were taken with an airborne system over a mature, humid tropical forest in the Brazilian Amazon

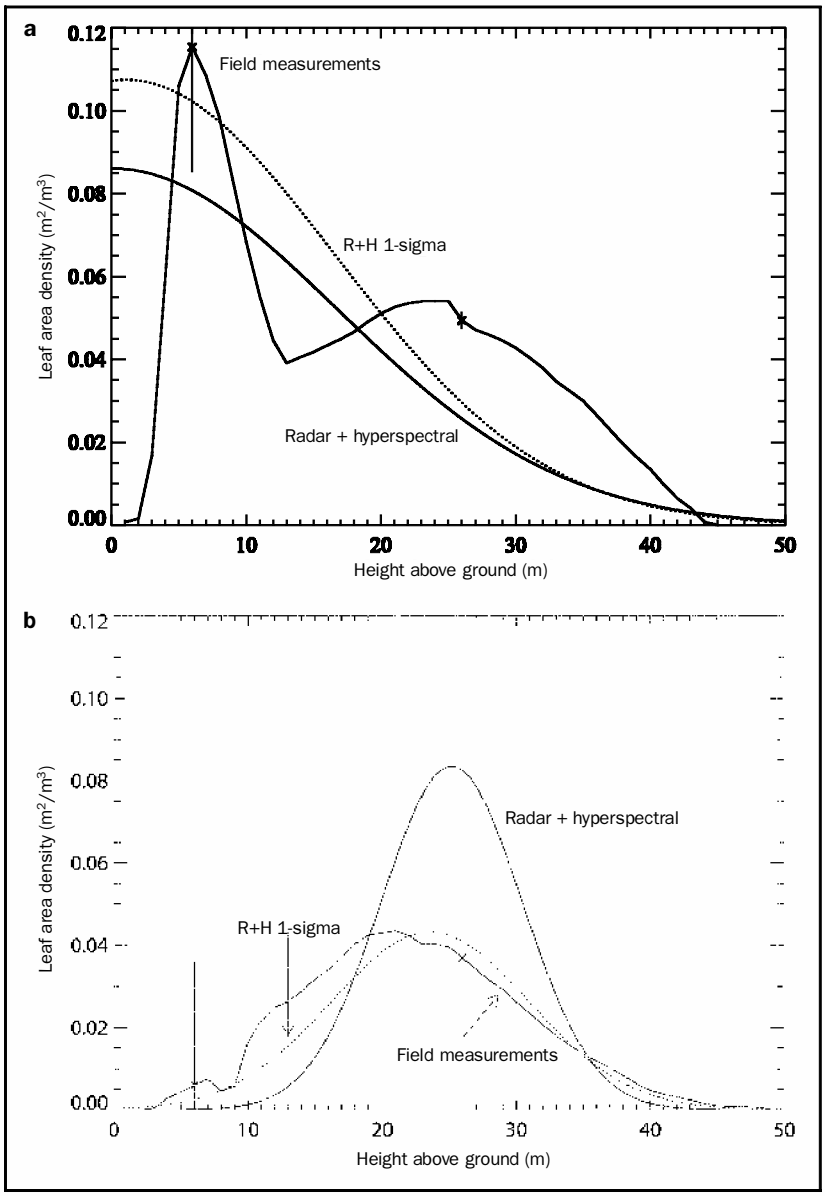

Figure 5. Remotely sensed leaf area density (LAD; square meters one-sided leaf area per cubic meter) as a function of height above the ground, generated from parameters estimated from airborne multiple-baseline C-band InSAR and normalized by hyperspectral leaf area indices. Data for radar and hyperspectral curves are from Treuhaft and colleagues (2002). "R+H 1-sigma" (dotted line) is the LAD profile generated by using values of InSAR and hyperspectral parameters one standard deviation away from the nominal estimates. Field measurements are also shown, with representative vertical error bars, at the asterisks indicating low and medium heights. (a) A multilayer plot of ponderosa pine in central Oregon, with sparse, tall old growth and dense, short young growth. (b) A plot of ponderosa pine in uniform, old-growth stands. The two different profiles are distinguished by the InSAR-based remotely sensed leaf area density. Reprinted, with permission, from the American Geophysical Union.

(Dutra et al. 2002), on transects 10 m × 100 m and 10 m × 250 m. These tests obtained 1- to 3-m accuracy in tree height. Other multiple-frequency demonstrations using Geographic Synthetic Aperture Radar, or GeoSAR, at P- and X-band frequencies produced 1- to 2-m agreement between multiple-frequency InSAR tree height determinations and those from field measurements over areas equivalent to the Amazon study (Siqueira et al. 2003). It is uncertain whether more complex profile parameters, as described in the next section, can be estimated with multiple-frequency InSAR.

Multiple-baseline interferometry. Multiple-baseline InSAR augments the single-baseline observations, once again creating multiple vector diagrams, or multiple mixtures of altitudes. Using the same fundamental principles that multiple-baseline radio astronomy applied to the structure of celestial radio sources (Thompson et al. 1986), multiple-baseline InSAR can potentially improve the accuracy of a simple structure profile, or it can enable the introduction of more profile parameters, describing more complex profiles. As the number of baselines increases to include a diversity of baseline lengths, the measured structure approaches the actual vegetation distribution, as conceptualized in figure 4. However, profiles corresponding to the coarser curves of figure 4 may be sufficient for estimating many biophysical quantities, such as biomass, as suggested by figure 5 and considerations in the section on ecosystem attributes. Biomass estimates can result from small numbers (1–2) of lidar statistics, potentially derivable from coarse profile characteristics, such as the height of median energy (HOME), as shown by Drake and colleagues (2002) for tropical forests. For some types of forests, the effective height produced by the single-baseline SRTM observation may serve a function similar to HOME and may suffice for biomass determination. Other experiments with lidar (Lefsky et al. 1999) and InSAR (Treuhaft et al. 2002) suggest that profile details beyond effective heights are required for biomass estimation. The degree to which increasing profile complexity improves biophysical products has not yet been studied thoroughly. Only the multiple-baseline augmentation, which may increase hardware costs for additional baselines (if they cannot be realized by repeat tracks), may be able to estimate the shapes of arbitrarily complex density profiles. The optimal number and lengths of baselines, frequencies, and polarizations, as well as possible fusion with other sensors, must be considered in the design of proposed multiple-baseline InSAR spaceborne sensors (Massonnet 2001).

A leaf area density, or LAD (one-sided leaf area per unit volume), profile was estimated for a 1-ha, multilayer plot of

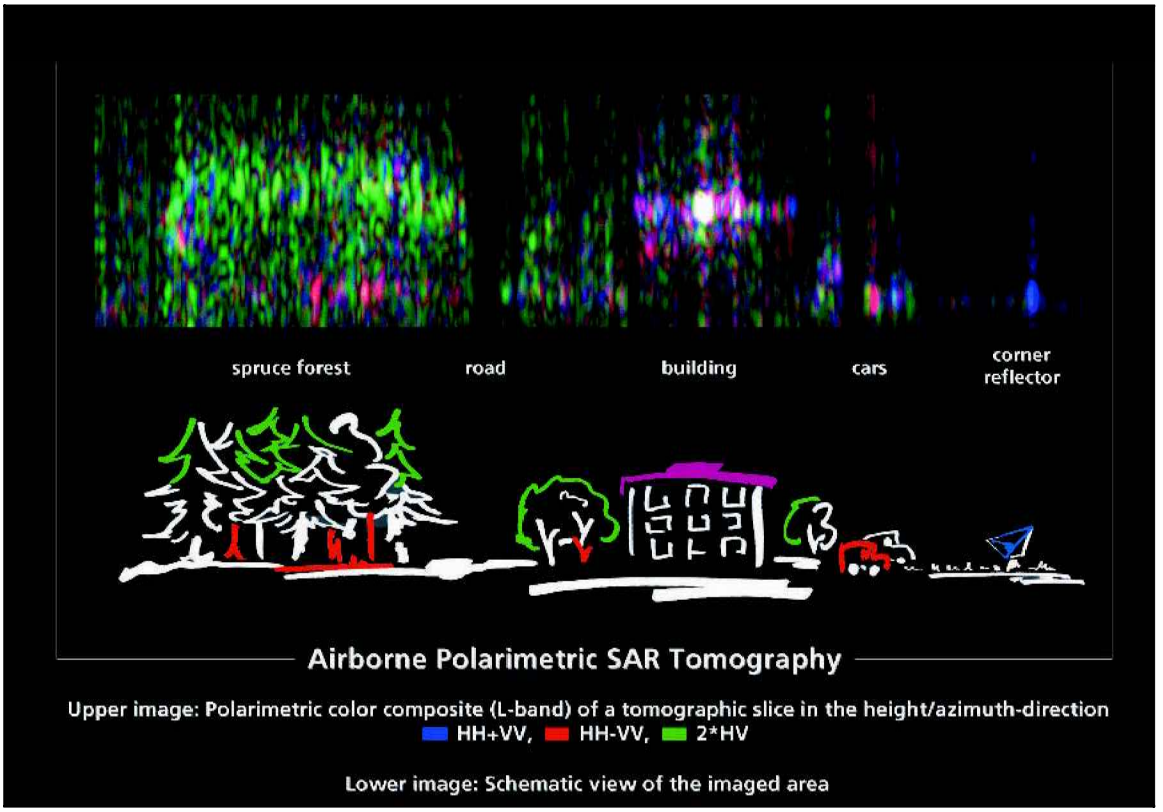

Figure 6. Tomographic intensity image from 14 airborne passes over a spruce forest and other objects as noted near Oberpfaffen, Germany (upper image). Schematic representation of the forest and ground objects (lower image). Colors in the upper image correspond to different polarization combinations in the data, and colors in the lower image correspond to expected polarization signatures of objects. Reprinted from Reigber and Moreira (2000), with permission. © 2000 Institute of Electrical and Electronics Engineers.

ponderosa pine in central Oregon from six C-band InSAR baselines using AIRSAR (figure 5a). The stand had sparse, tall old growth and dense, short young growth. A total of 12 interferometric observations (one amplitude and phase per baseline) (Treuhaft et al. 2002) produced the relative LAD profile, that is, LAD as a function of altitude with an undetermined overall normalization factor. A field-measured LAD is also shown as the curve with vertical error bars through the asterisks at low and medium altitude (figure 5a). A Gaussian model profile with two parameters, the center and standard deviation, yielded the relative densities shown in figure 5a. The two radar and hyperspectral (R+H) curves are normalized with parameters from hyperspectral data (discussed in the section below on data fusion). Figure 5b shows a second stand of ponderosa pine, but unlike the mixed-age stand of figure 5a, this stand is uniform old growth. Its field-measured leaf area density is broad and peaked at the center of the nearly symmetric distribution, unlike the low-altitude peak in figure 5a.

The R+H 1-sigma curves in figure 5 are within one standard deviation of the field measurements for much of the range of height above ground. The remote sensing curves reproduce the coarse features of the field LAD and clearly distinguish between the two very different LAD profiles of the mixed and uniform stand. Coarse features of the LADs for nine other stands (not shown here) correlated well with field estimates of LAD and tree-height statistics. However, figure 5 also shows how a few baselines constrain InSAR to miss some details of the profile, reminiscent of the "few-baseline" schematic profile of figure 4. Increasing the number of baselines as well as addressing instrumental issues in the AIRSAR data set potentially will improve the performance of InSAR-based LAD. Future experiments must evaluate the trade-off between number of baselines and vertical resolution for producing ecosystem attributes of interest to ecologists, such as biomass.

The only other published demonstration of microwave vegetation profiling is by tomography, which is related to multiple-baseline interferometry (Reigber and Moreira 2000). Tomographic profiles achieved with 14 different airplane overflights in Oberpfaffenhofen, Germany, showed clear correlations with vegetation vertical structure features, as well as with features of buildings and road surfaces. From qualitative images (figure 6), the many baselines afforded by 14 overflights appear to yield a vertical resolution possibly better than that of figure 5—the many-baseline profiles, like lidar profiles, were not constrained to be Gaussian.

Combining InSAR with optical remote sensing

Global remote sensing of forest structure requires unambiguous measurements of forests with diverse canopy architectures; species; and climatic, topographic, and edaphic conditions. Just as multiple polarizations, frequencies, and baselines improve InSAR's accuracy, it is likely that the fusion of the outputs of InSAR with those of several other types of sensors will deliver the most robust and accurate forest structure estimates. This section suggests general considerations and frameworks with which to envision fusion scenarios for InSAR and optical sensors for structure monitoring. Much of the general discussion also applies to fusion of InSAR with other microwave sensors or ancillary data types.

While InSAR density profiles scale with biophysical quantities such as vertical leaf area distribution, spectroscopic data provide a more direct measurement of the biophysical contents of the target, but not necessarily the vertical distribution of the contents. Optical techniques also respond in varying degrees to structural characteristics. We therefore propose two potential modes of fusing InSAR with optical sensors: (1) using the complementary dependence of the optical data on biophysical characteristics to relate the structural density profiles from InSAR to biophysical profiles, a method we call "biophysical fusion," and (2) using the optical sensitivity to structure to improve the accuracy or resolution of the InSAR profiles through "structural fusion." Spectroscopic sensors (optical sensors that acquire radiance data for different wavelengths) favor the former and lidar the latter, but both may be considered for all sensors. Our description of biophysical and structural fusion will focus on spectroscopic (primarily hyperspectral) and lidar remote sensing, respectively.

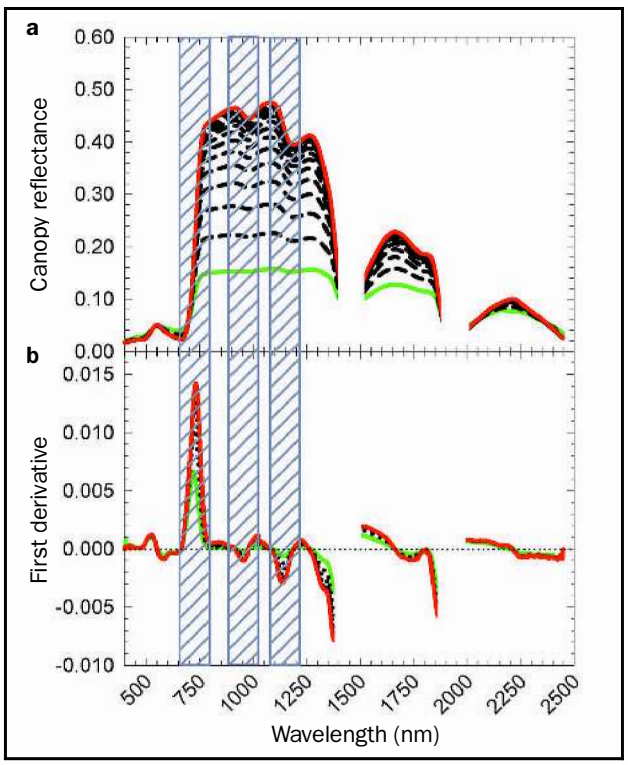

Figure 7. Calculated hyperspectral reflectance (top) and the reflectance derivative (bottom) as a function of wavelength for different values of leaf area index (LAI), starting with 0.5 (green line) and increasing in increments of 0.5 (dashed lines) up to 8.0 (red line). Sensitivities of both the reflectance and the derivative, primarily in each of the gray, hatched wavelength regions (680–760 nanometers [nm], 900–1050 nm, and 1100–1250 nm) are used to estimate LAI. Other regions of the spectrum show less sensitivity to variations in LAI beyond values of about 1 to 2.

Spectroscopic fusion. Imaging spectroscopy, also known as hyperspectral imaging, is the measurement of solar radiation reflected from the Earth's surface in contiguous, narrow spectral channels spanning the wavelength region from 0.4 to 2.5 μm (micrometers). The high number of spectral channels (> 200) allows identification of materials with overlapping, but distinct, spectral signatures (Ustin et al. 2004). Hyperspectral observations can detect variation in canopy leaf area index (LAI), with upper limits in the range of 6 to 10, through a combination of spectral derivatives centered at the 0.97- and 1.2-μm regions (near-infrared) and across the 0.69- to 0.71-μm range (red; Asner 1998, Roberts et al. 1998, Ustin et al. 1998).

Two measures of hyperspectral imaging, the reflectance and reflectance derivative, change in response to increases in LAI (Asner 1998), as shown in figure 7. When estimated with a model of the hyperspectral reflectance and reflectance derivative, LAI can be used to normalize the InSAR vertical density profile. That is, the LAI from optical measurements introduces greater biophysical meaning to the relative density produced by InSAR. This biophysical fusion mode yielded the LAD as a function of height above the surface of two ponderosa pine stands in central Oregon (figure 5; Treuhaft et al. 2002). The structural signatures in hyperspectral data can also be used to enhance the structural information of InSAR. For example, when a forest is disturbed, a significant amount of nonphotosynthetic vegetation (e.g., surface litter, wood) and bare soils can be exposed, changing the hyperspectral response shown in figure 7.

Another type of spectroscopic instrument, the multiangle imaging spectroradiometer (MISR) (Diner et al. 1998), can conceivably contribute to a fusion scenario with InSAR. MISR has four radiometric channels from about 0.44 to 0.86 μm and nine view angles. Structural properties have been inferred from MISR data (Gobron et al. 2002), and it is possible that MISR may work with InSAR in the future in some combination of the biophysical and structure fusion modes.

Lidar fusion. As noted above, lidar and InSAR have complementary strengths, which may potentially be combined. The lidar profiles may set limits on InSAR parameter estimation and improve the accuracy of the broad spatial estimates derived with InSAR. A few very accurate lidar profiles

sampled within the InSAR swath may reduce the number of baselines required for InSAR spaceborne sensors.

Airborne structural fusion of InSAR and lidar yielded optimal coverage and accuracy in tree heights (Slatton et al. 2001). Fusion of InSAR with lidar improved the accuracy of tree heights determined from two InSAR baselines by factors of two to three, and meter-level accuracies resulted over areas of about 1 ha. Lidar was flown in multiple strips over these areas, with a few-meter spot size. Demonstrations of the optimal modes of combining InSAR and lidar for full profiles do not yet exist.

Ecosystem attributes from vegetation profiles

We have established that InSAR's vertical profiles of vegetation can be enhanced in combinations with other sensors. Here we discuss other ecosystem attributes that can be estimated from these profiles. For example, within a canopy, the vertical distribution of foliage determines the pattern of light availability, controlling processes such as leaf development, leaf energy balance, water use, photosynthesis (Norman and Campbell 1991, Ellsworth and Reich 1993), and carbon and nutrient cycling within ecosystems. Radiative transfer models characterize the effects of canopy structure on diffuse and direct radiation and thus photosynthetic efficiency, which can affect the rate of carbon uptake by vegetation (Law et al. 2001). Some physiological process models require structural profiles to simulate the soil–vegetation–atmosphere exchange of carbon dioxide and water vapor by means of photosynthesis, evapotranspiration, and respiration (Williams et al. 2001). Such models quantify changes in productivity and carbon storage with interannual variation in climate, growth stage, and disturbance. Vertical profiles of vegetation can also be useful for investigating the biological diversity of plants and animals in relation to structural diversity or productivity.

The 3-D remote sensing of structure prompts investigation of the dependence of biomass on structural parameters. Allometric relations currently being explored, which relate biomass to 3-D structural information from InSAR and lidar, may ultimately be robust for global biomass monitoring (Lefsky et al. 1999, Drake et al. 2002, Treuhaft et al. 2003). As an example, biomass estimates for 11 stands of ponderosa pine, grand fir, and larch resulted from remotely sensed LAD (figure 5) in central Oregon (Treuhaft et al. 2003). Rather than relate biomass to tree height and diameter, as is done with field measurements, new allometrics, which are functions of LAI and the mean and standard deviation of the InSAR-derived density distribution, were used to determine biomass (figure 8). The field estimates are plotted against the best-fit remote sensing estimates of biomass. The scatter of remote sensing estimates about field estimates is 25 megagrams (Mg) per ha, or about 16% of the average stand biomass, for stands up to 300 Mg per ha, showing no signs of the "saturation" at about 100 Mg per ha usually associated with C-band power biomass estimation. The 25 Mg-per-ha scatter is competitive with some of the best published biomass results from lidar (about 20 Mg per ha for biomasses up to 250 per ha) (Drake et al. 2002). The scatter is dominated by field measurement error of about 15% and far exceeds the 45-Mg-per-ha performance of C-band power-based biomass estimates from the same data set. InSAR's direct sensitivity to structure accounts in part for the improved biomass performance. Additionally, at high biomasses, InSAR is not nearly as prone to the biomass saturation phenomenon as radar power, because of its signal and noise characteristics (Treuhaft and Siqueira 2004).

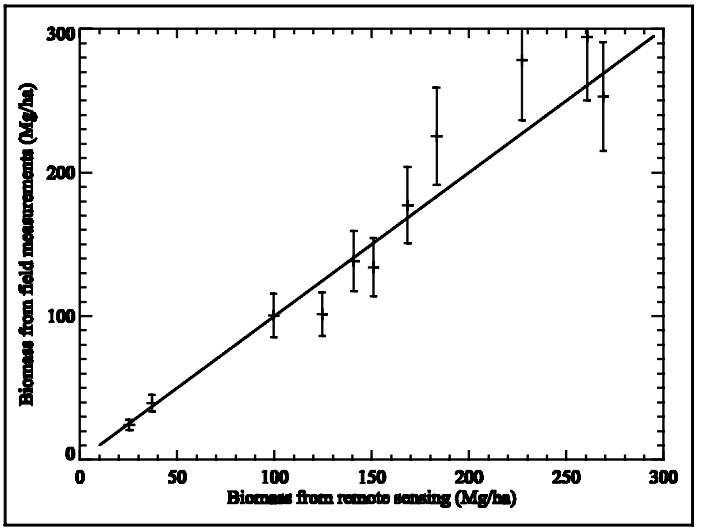

Figure 8. Field-measured biomass versus biomass from leaf area density profiles (such as figure 5) from InSAR, normalized by hyperspectral data. The scatter about the y = x *line is 25 megagrams per hectare, or about 16% of the average biomass. Two parameters were adjusted to fit the remotely sensed biomasses to the field biomasses. Although two parameters were estimated from 11 observations, accuracy is highly significant, with greater than 99.5% confidence. Reprinted from Treuhaft and colleagues (2003), with permission from the American Geophysical Union.*

Prospects for global InSAR forest monitoring

As a new application to forest profiling, InSAR shows promise for enabling 3-D microwave remote sensing of forests, which may improve our understanding of the carbon cycle and other forest ecological processes. InSAR produces tree height measurements as well as LAD, in concert with hyperspectral data, and both LAD and derived biomass estimates are critical to understanding vegetation dynamics and global carbon sequestration. Spaceborne interferometry can operate in all weather conditions, sampling swaths up to 80 km, providing vertical structure measurements with 0.25-ha to 1-ha lateral resolution. The InSAR coverage for heights or full profiles is orders of magnitude better than proposed or flying spaceborne lidars.

InSAR meets two proposed criteria of sensitivity and estimability of vertical structure; however, InSAR satisfies the latter criterion only with multiple-polarization, multiple-

frequency, or multiple-baseline data, the last of which can estimate full vegetation profiles (as opposed to vegetation heights). Multiple-polarization or multiple-frequency systems will probably best deliver tree height. Multiple-baseline InSAR produces complete profiles, but for small numbers of baselines, InSAR's full-profile vertical accuracy is coarser than that of lidar, which is a more direct measurement of the vertical distribution of forest vegetation. Hyperspectral or multispectral or possibly multiangle optical observations, combined with InSAR, lend more biophysical meaning to InSAR relative density profiles, and they can also improve the accuracy of structure estimates. Combining InSAR's potential as a gapless global monitoring tool with that of sparse but highly accurate spaceborne lidar profiles may constitute an optimal data fusion strategy for global 3-D forest structure.

Future spaceborne InSAR profiling missions will probably require multiple baselines (Massonet 2001) and possibly multiple polarizations and frequencies. Airborne InSAR and optical experiments over diverse forest types, along with accurate field measurements, will supply ecologists with the scope of possibilities for global 3-D forest monitoring. From these possibilities, the needs and applications for profiles, as articulated by ecologists, can then substantially guide future InSAR spaceborne designs.

Acknowledgments

We very appreciatively acknowledge Richard Waring's invaluable, detailed readings of the manuscript and numerous clarifying suggestions for textual revision. We further thank Warren Cohen, guest editor of the special section on remote sensing, for extensive comments on the manuscript. We also thank the anonymous reviewers for many helpful suggestions. We gratefully acknowledge the support of the Terrestrial Ecology Program, managed by Diane Wickland for the National Aeronautics and Space Administration's Earth Science Enterprise (grant no. NAG5-8315). The research described in this article was carried out in part by the Jet Propulsion Laboratory, California Institute of Technology, under contract with NASA.

References cited

Asner GP. 1998. Biophysical and biochemical sources of variability in canopy reflectance. Remote Sensing of Environment 64: 234–253.

———. 2001. Cloud cover in Landsat observations of the Brazilian Amazon. International Journal of Remote Sensing 22: 3855–3862.

Cloude SR, Papathanassiou KP. 1998. Polarimetric SAR interferometry. IEEE Transactions on Geoscience and Remote Sensing 36: 1551–1565.

Cohen WB, Goward SN. 2004. Landsat's role in ecological applications of remote sensing. BioScience 54: 535–545.

Diner DJ, et al. 1998. Multi-angle Imaging SpectroRadiometer (MISR) instrument description and experiment overview. IEEE Transactions on Geoscience and Remote Sensing 36: 1072–1087.

Drake JB, Dubayaha RO, Clark DB, Knox RG, Blair JB, Hofton MA, Chazdone RL, Weishampel JF, Prince SD. 2002. Estimation of tropical forest structural characteristics using large-footprint lidar. Remote Sensing of Environment 79: 305–319.

Dutra LV, Elmiro MT, Soares BS, Mura FJC, Santos JR, Freitas CC, Araujo LS, de Albuquerque PCG, Vieira PR, Gama FF. 2002. Assessment of digital elevation models obtained in Brazilian Amazon based on P and X band airborne interferometric data. Pages 3617–3619 in IGARSS 2002: Remote Sensing, Integrating Our View of the Planet. Proceedings of the IEEE International Geoscience and Remote Sensing Symposium and 24th Candian Symposium on Remote Sensing, Westin Harbor Castle, Toronto, Canada, 24–28 June 2002, vol. 6. New York: Institute of Electrical and Electronics Engineers.

Ellsworth DS, Reich PB. 1993. Canopy structure and vertical patterns of photosynthesis and related leaf traits in a deciduous forest. Oecologia 96: 169–178.

Gardner CS. 1992. Ranging performance of satellite laser altimeters. IEEE Transactions on Geoscience and Remote Sensing 30: 1061–1072.

Gobron NB, Pinty B, Verstraete MM, Widlowski JL, Diner DJ. 2002. Uniqueness of multiangular measurements, pt. II: Joint retrieval of vegetation structure and photosynthetic activity from MISR. IEEE Transactions on Geoscience and Remote Sensing 40: 1574–1592.

Graham LC. 1974. Synthetic interferometer radar for topographic mapping. Proceedings of the IEEE 62: 763–768.

Hagberg JO, Ulander LMH, Askne J. 1995. Repeat-pass SAR interferometry over forested terrain. IEEE Transactions on Geoscience and Remote Sensing 33: 331–340.

Harding DJ, Lefsky MA, Parker GG, Blair JB. 2001. Laser altimeter canopy height profiles: Methods and validation for closed-canopy, broadleaf forests. Remote Sensing of Environment 76: 283–297.

Hofton MA, Rocchio LE, Blair JB, Dubayah R. 2002. Validation of vegetation canopy lidar sub-canopy topography measurements for a dense tropical forest. Journal of Geodynamics 34: 491–502.

Igarashi T. 2001. ALOS mission requirement and sensor specifications. Advances in Space Research 28: 127–131.

Law BE, Cescatti A, Baldocchi DD. 2001. Leaf area distribution and radiative transfer in open-canopy forests: Implications to mass and energy exchange. Tree Physiology 21: 777–787.

Law BE, Sun O, Campbell J, Van Tuyl S, Thornton P. 2003. Changes in carbon storage and fluxes in a chronosequence of ponderosa pine. Global Change Biology 9: 510–524.

Law BE, Turner DP, Lefsky M, Campbell J, Guzy M, Sun O, Van Tuyl S, Cohen WB. Carbon fluxes across regions: Observational constraints at multiple scales. In Wu J, Jones B, Li H, Loucks O, eds. Scaling and Uncertainty Analysis in Ecology: Methods and Applications. New York: Columbia University Press. Forthcoming.

Lefsky MA, Cohen WB, Acker SA, Parker GG, Spies TA, Harding D. 1999. Lidar remote sensing of the canopy structure and biophysical properties of Douglas-fir western hemlock forests. Remote Sensing of Environment 70: 339–361.

Lefsky MA, Cohen WB, Parker GG, Harding DJ. 2002. Lidar remote sensing for ecosystem studies. BioScience 52: 19–30.

Luckman A, Baker J, Wegümller U. 2000. Repeat-pass interferometric coherence measurements of disturbed tropical forest from JERS and ERS satellites. Remote Sensing of Environment 73:350–360.

Marchak MP. 1995. Logging the Globe. Quebec: McGill-Queen's University Press.

Massonnet D. 2001. The interferometric cartwheel: A constellation of passive satellites to produce radar images to be coherently combined. International Journal of Remote Sensing 22: 2413–2430.

Nilsson M. 1996. Estimation of tree heights and stand volume using an airborne lidar system. Remote Sensing of Environment 56: 1–7.

Norman JM, Campbell GS. 1991. Canopy structure. Pages 301–325 in Ehlringer J, Mooney HA, Pearcy RW, Rundel P, eds. Physiological Plant Ecology: Field Methods and Instrumentation. London: Chapman and Hall.

Papathanassiou KP, Cloude SR. 2001. Single-baseline polarimetric SAR interferometry. IEEE Transactions on Geoscience and Remote Sensing 39: 2352–2363.

Pielke RA, Avissar R. 1990. Influence of landscape structure on local and regional climate. Landscape Ecology 4: 133–155.

Pulliainen J, Engdahl M, Hallikainen M. 2003. Feasibility of multi-temporal interferometric SAR data for stand-level estimation of boreal forest stem volume. Remote Sensing of Environment 85: 397–409.

Rabus B, Eineder M, Roth A, Bamler R. 2003. The shuttle radar topography mission: A new class of digital elevation models acquired by spaceborne radar. Journal of Photogrammetry and Remote Sensing 57: 241–262.

Reigber A, Moreira A. 2000. First demonstration of airborne SAR tomography using multibaseline L-band data. IEEE Transactions on Geoscience and Remote Sensing 38: 2142–2152.

Roberts DA, Gardner M, Church R, Ustin S, Scheer G, Green RO. 1998. Mapping chaparral in the Santa Monica Mountains using multiple endmember spectral mixture models. Remote Sensing of Environment 65: 267–279.

Rodriguez E, Martin JM. 1992. Theory and design of interferometric synthetic aperture radars. Proceedings of the International Conference on Information and Knowledge Engineering 139: 147–159.

Rosen PA. Hensley S, Joughin IR, Li FK, Madsen SN, Rodriguez E, Goldstein RM. 2000. Synthetic aperture radar interferometry. Proceedings of the IEEE 88: 333–382.

Schlesinger WH. 1991. Biogeochemistry: An Analysis of Global Change. San Diego: Academic Press.

Siqueira P, Hensley S, Rodriguez E, Simard M. 2003. X/P-merge software for estimating vegetation height. NASA Tech Brief NPO-40268.

Slatton KC, Crawford MM, Evan BL. 2001. Fusing interferometric radar and laser altimeter data to estimate surface topography and vegetation heights. IEEE Transactions on Geoscience and Remote Sensing 39: 2470–2482.

Thompson AR, Moran JM, Swenson GW Jr. 1986. Interferometry and Synthesis in Radio Astronomy. New York: John Wiley and Sons.

Treuhaft RN, Siqueira PR. 2000. Vertical structure of vegetated land surfaces from interferometric and polarimetric radar. Radio Science 35: 141–177.

———. 2004. The calculated performance of forest structure and biomass from interferometric radar. Waves in Random Media 14: S345–S358.

Treuhaft RN, Madsen SN, Moghaddam M, Van Zyl JJ. 1996. Vegetation characteristics and surface topography from interferometric radar. Radio Science 31: 1449–1485.

Treuhaft RN, Asner GP, Law BE, Van Tuyl S. 2002. Forest leaf area density profiles from the quantitative fusion of radar and hyperspectral data. Journal of Geophysical Research 107: 4568–4580.

Treuhaft RN, Asner GP, Law BE. 2003. Structure-based forest biomass from fusion of radar and hyperspectral observations. Geophysical Research Letters 30: 1472–1475.

Ustin SL, Roberts DA, Pinzon J, Jacquemoud S, Gardner M, Scheer G, Castaneda CM, Palacios-Orueta A. 1998. Estimating canopy water content of chaparral shrubs using optical methods. Remote Sensing of Environment 65: 280–291.

Ustin SL, Roberts DA, Gamon JA, Asner GP, Green RO. 2004. Using imaging spectroscopy to study ecosystem processes and properties. BioScience 54: 523–534.

Wagner W, et al. 2003. Large-scale mapping of boreal forest in SIBERIA using ERS tandem coherence and JERS backscatter data. Remote Sensing of Environment 85: 125–144.

Waring RH, Running SW. 1998. Forest Ecosystems: Analysis at Multiple Scales. San Diego: Academic Press.

Waring RH, Way JB, Hunt ER, Morrissey L, Ranson KJ, Weishampel JF, Oren R, Franklin SE. 1995. Imaging radar for ecosystem studies. BioScience 45: 715–723.

Wegmüller U, Werner C. 1997. Retrieval of vegetation parameters with SAR interferometry. IEEE Transactions on Geoscience and Remote Sensing 35: 18–24.

Williams M, Law BE, Anthoni PM, Unsworth MH. 2001. Using a simulation model and ecosystem flux data to examine carbon-water interactions in ponderosa pine. Tree Physiology 21: 287–298.

Zwally HJ, et al. 2002. ICESat's laser measurements of polar ice, atmosphere, ocean, and land. Journal of Geodynamics 34: 405–445.